



OPEN

CONFERENCE  
PROCEEDINGS

ISFM2014

.....

SUBJECT AREAS:

SOFT MATERIALS

BIOPHYSICAL CHEMISTRY

Received  
7 October 2014Accepted  
5 January 2015Published  
23 March 2015

Correspondence and  
requests for materials  
should be addressed to  
J.-H.B. (jhboo@skku.  
edu)

# Micropatterning of TiO<sub>2</sub> Thin Films by MOCVD and Study of Their Growth Tendency

Ki-Hwan Hwang<sup>1</sup>, Byung-Chang Kang<sup>1</sup>, Duk Young Jung<sup>1</sup>, Youn Jea Kim<sup>2</sup> & Jin-Hyo Boo<sup>1</sup><sup>1</sup>Department of Chemistry, Sungkyunkwan University, Suwon 440-746, Korea, <sup>2</sup>Department of Mechanical Engineering, Sungkyunkwan University, Suwon 440-746, Korea.

In this work, we studied the growth tendency of TiO<sub>2</sub> thin films deposited on a narrow-stripe area (<10 μm). TiO<sub>2</sub> thin films were selectively deposited on OTS patterned Si(100) substrates by MOCVD. The experimental data showed that the film growth tendency was divided into two behaviors above and below a line patterning width of 4 μm. The relationship between the film thickness and the deposited area was obtained as a function of  $f(x) = a[1 - e^{(-bx)}]c$ . To find the tendency of the deposition rate of the TiO<sub>2</sub> thin films onto the various linewidth areas, the relationship between the thickness of the TiO<sub>2</sub> thin film and deposited linewidth was also studied. The thickness of the deposited TiO<sub>2</sub> films was measured from the alpha-step profile analyses and cross-sectional SEM images. At the same time, a computer simulation was carried out to reveal the relationship between the TiO<sub>2</sub> film thickness and deposited line width. The theoretical results suggest that the mass (velocity) flux in flow direction is directly affected to the film thickness.

The patterning of thin films is of considerable scientific and technological interest. Various ways to obtain micro patterns of thin films have been thoroughly investigated. The current common methods of patterned thin film production are photolithography and etching, in which the films are deposited on the entire areas of the substrates and partially removed using other processes. These methods need high energy and many steps to produce the final products. Soft lithography is a method of making micro size patterns and structures simply using organic materials without involving high energy<sup>1</sup>. In particular, micro-contact printing (μCP) is a very convenient and non-photolithographic technique that can generate patterned features of self-assembled monolayers (SAMs) on various substrates<sup>2-4</sup>. The μCP technique allows hydrophobic patterns with micron dimensions to be formed on hydrophilic surfaces, thus avoiding the use of photolithographic-type procedures. Such techniques make it possible to fabricate devices that can be used in optical communications or biochemical research. We firstly performed the micro-patterning of TiO<sub>2</sub> thin films on OTS patterned Si(100) substrates by the MOCVD method and studied their characteristics<sup>5</sup>. We found that the micro-contact printing technique could be applied to micro-electromechanical systems (MEMS), sensors and microelectronics with large patterning features on the micrometer scale. Small-area (<4" wafer) and larger (>1 μm) line-widths are perfectly suited for most applications of MEMS<sup>6</sup>. In order to combine the advantages of MOCVD and micro-contact printing, it is necessary to study the growth tendency of thin films deposited on various feature sizes.

Crystal growth theory and models such as classical two dimensional nucleation theory, screw dislocation theory, classical nucleation theory, chemical bonding theory, and reaction rate models as well as mass & heat transfer models were proposed to depict the crystal growth process in both nano- and bulk-regimes<sup>7-9</sup>. Among those theories and models, the chemical bonding theory based on calculation and simulation was applied to growth both nano-crystals and bulk-crystals<sup>9,10</sup>. From experimental point of view, the Czochralski (Cz) technique is the conventional method for growing single crystals, while both PVD and CVD techniques are common method for growing thin films and nano-crystals. In general, decreasing growth rate, decreasing gas pressure of the growth atmosphere were the main practical processing parameters together with temperature. However, there are not many theoretical and experimental data on the study about the relationship between film thickness (i.e. dependence on gas flux velocity & pressure) and submicro-patterned line width (inside or outside channels).

In the present study, TiO<sub>2</sub> thin films were selectively deposited on Si(100) substrates whose surfaces were OTS patterned with various feature sizes. The focus of this work is the study of the growth tendency of TiO<sub>2</sub> thin films deposited on Si(100) substrates whose surfaces were patterned with sizes of 10 μm and less.

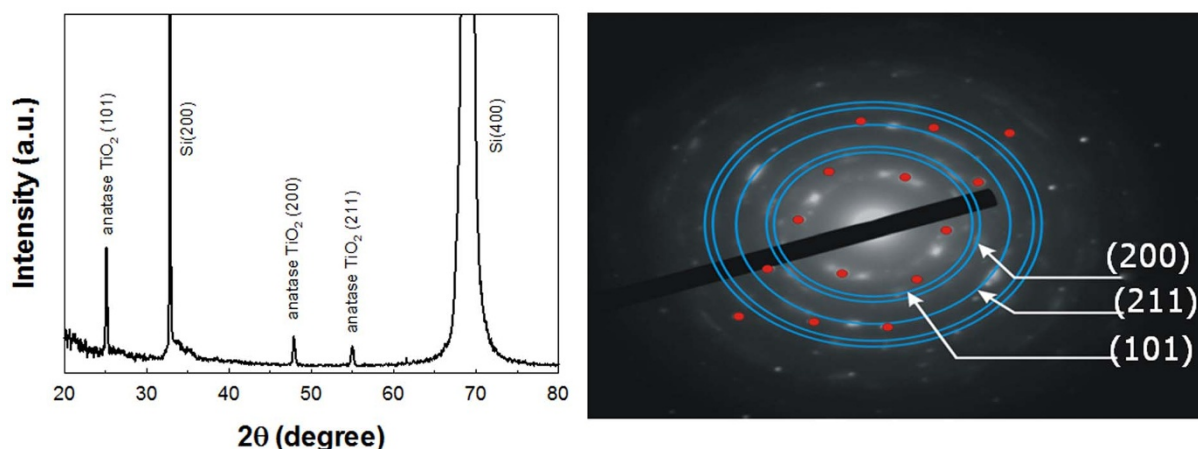


**Figure 1** | Typical XRD pattern(left) and TED pattern(right) of a  $\text{TiO}_2$  thin film grown on bare Si(100) substrate at  $350^\circ\text{C}$  by MOCVD method.

## Results and Discussion

Figure 1 shows a typical XRD pattern(left) of a  $\text{TiO}_2$  thin film grown on Si(100) substrate at  $350^\circ\text{C}$  by MOCVD method. Three diffracted peaks were clearly observed at  $2\theta = 25, 48, 55$  degrees which attributed to anatase type  $\text{TiO}_2(101)$ , (200), and (211) diffracted planes, respectively. Among three peaks, the  $\text{TiO}_2(101)$  peak was the major one, indicating that a highly oriented polycrystalline film was obtained and the main growth direction of  $\text{TiO}_2$  crystals was [101] direction. Because all films have grown below  $400^\circ\text{C}$  to avoid destruction of the OTS SAMs layer, only anatase  $\text{TiO}_2$  phase with the same film growth direction was obtained in this work. This was also confirmed with TED pattern [shown in right-hand side of the figure 1] that obtained from the same film. Figure 2 shows HRTEM image(a) as well as cross-sectional TEM image(b). From the HRTEM image, we could confirm that high quality film was obtained even though there are some defects in the  $\text{TiO}_2$  film layers. Also, from the inset of figure 2(a), we calculated a lattice spacing of  $0.209$  nm that is correlated with that of reference data of anatase  $\text{TiO}_2$ . Based on the cross-sectional TEM image, at least, we could claim that there are no cracks on the  $\text{TiO}_2$  surface and the interface between  $\text{TiO}_2$  film and Si substrate is very sharp, signifying no inter-diffusion between  $\text{TiO}_2$  and Si. Figure 3 shows wide area SEM image(left), narrow area SEM image(middle), and high resolution SEM image(right) which obtained from the  $\text{TiO}_2$  film layer after further zoom in the middle SEM image. With these images, we could make a conclusion that  $\text{TiO}_2$  film was grown only on the bare Si surface selectively and there was no  $\text{TiO}_2$  on OTS SAMs region.

The as-deposited  $\text{TiO}_2$  thin films were characterized by an alpha-step profiler. Figure 4(a) shows the alpha-step profile result of the

deposited  $\text{TiO}_2$  thin film on the Si(100) substrate whose surface was patterned with Pattern (1). Figure 4(b) shows the shape of the  $\text{TiO}_2$  thin film deposited on the patterned Si(100) surface, as shown in Pattern (2). In both cases, the interfaces between the  $\text{TiO}_2$  deposition and OTS SAMs areas showed nearly vertical shapes, indicating that  $\text{TiO}_2$  was selectively deposited on the OTS uncovered Si(100) surface area. However, a difference in thickness was observed in Figure 4(a), indicating that the thickness of the deposited  $\text{TiO}_2$  increases with increasing line-width up to  $4\ \mu\text{m}$ , while there is no change in the height of the  $\text{TiO}_2$  thin films with a line-width of more than  $4\ \mu\text{m}$ . On the other hand, the same deposition thickness of about  $100$  nm is observed in Figure 4(b), signifying that the spaces between the parallel lines do not influence the deposition rate. Figure 5 shows the high resolution alpha-step profile results of the  $\text{TiO}_2$  thin films. The difference of deposition height is clearly shown. Also, the deposition morphologies and thickness were confirmed by using SEM analyses. Figure 6 shows SSEM images of the  $\text{TiO}_2$  thin films deposited on the substrates with difference line-widths. We confirmed once more the difference in the growth rate depending on the line-width and that the boundaries between the OTS SAMs and  $\text{TiO}_2$  deposited areas had very clear shapes. Moreover, the AFM analyses supported the selectivity and difference in growth rate with the different line-widths. Figure 7 shows the 3D AFM images of the  $\text{TiO}_2$  thin films deposited on the OTS patterned Si(100) surfaces. To find the variation of the deposition rate of the  $\text{TiO}_2$  thin films with the line-width, the relationship between the  $\text{TiO}_2$  thin film thickness and deposited line-width was studied. The thickness of the deposited  $\text{TiO}_2$  films was measured from the alpha-step profile analyses and cross-sectional SEM images. Figure 8 shows the tendency of film growth as a

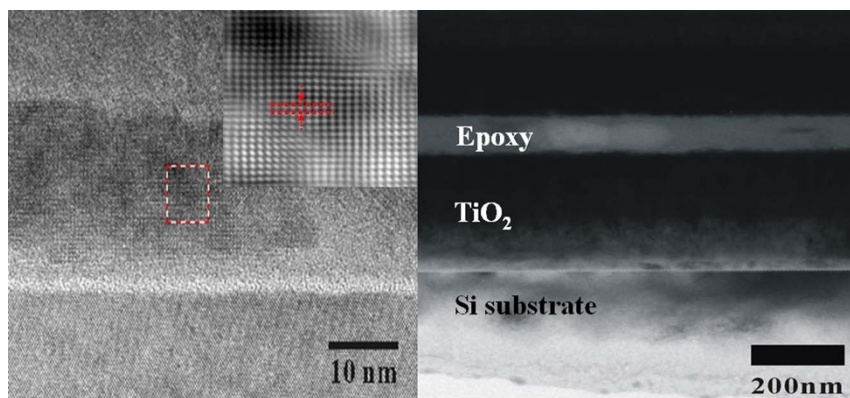


**Figure 2** | HRTEM image(a) as well as cross-sectional TEM image(b) of the same  $\text{TiO}_2$  film as the Figure 1. Inset of Figure 2(a) shows high resolution image of a selected area (marked with dashed lines).

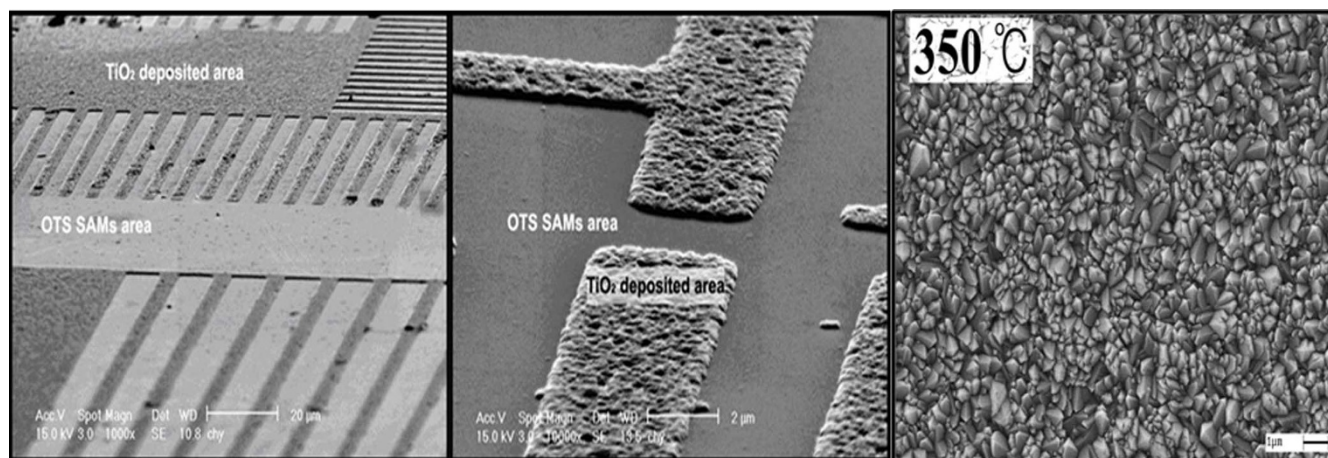


**Figure 3** | Wide area SEM image(left), narrow area SEM image(middle), and high resolution SEM image(right) which obtained from the  $\text{TiO}_2$  film layers after further zoom in the middle SEM image.

function of the deposition time. It can be seen that two different growth tendencies are observed. At line-widths of less than approximately  $4 \mu\text{m}$ , the growth rate increased with increasing line-width, while at line-widths above  $4 \mu\text{m}$  the growth rate remained almost the same. Based on these results, this growth tendency can be fitted by the following function.

$$f(x) = a \left[ 1 - e^{(-bx)} \right] c \quad (1)$$

where  $x$  is the line-width of the deposited  $\text{TiO}_2$  and  $a$ ,  $b$  and  $c$  are constants.

Y. Sakata, et al.<sup>11</sup> reported that the migration from the masked region and lateral vapor-phase diffusion are the mechanism of

growth-rate enhancement for selective metal-organic chemical vapor deposition. There are two additional source supply paths for selective MOCVD. The first one is the migration from the masked region (MMR) where the source materials migrate from the mask (OTS SAMs area in our case) region to the growth region. The other is lateral vapor-phase diffusion (LVD) where the source materials laterally diffuse from the masked region to the growth region in the vapor phase. The authors reported that in wide-stripe selective CVD, where the layers are grown in more than  $5\text{--}10 \mu\text{m}$ -wide stripe regions, the MMR effect is negligible, because the species that migrate from the masked region move only a few microns at most on the semiconductor surface and create the edge growth region. Thus, the LVD effect is the **only** major mechanism for the center region of wide

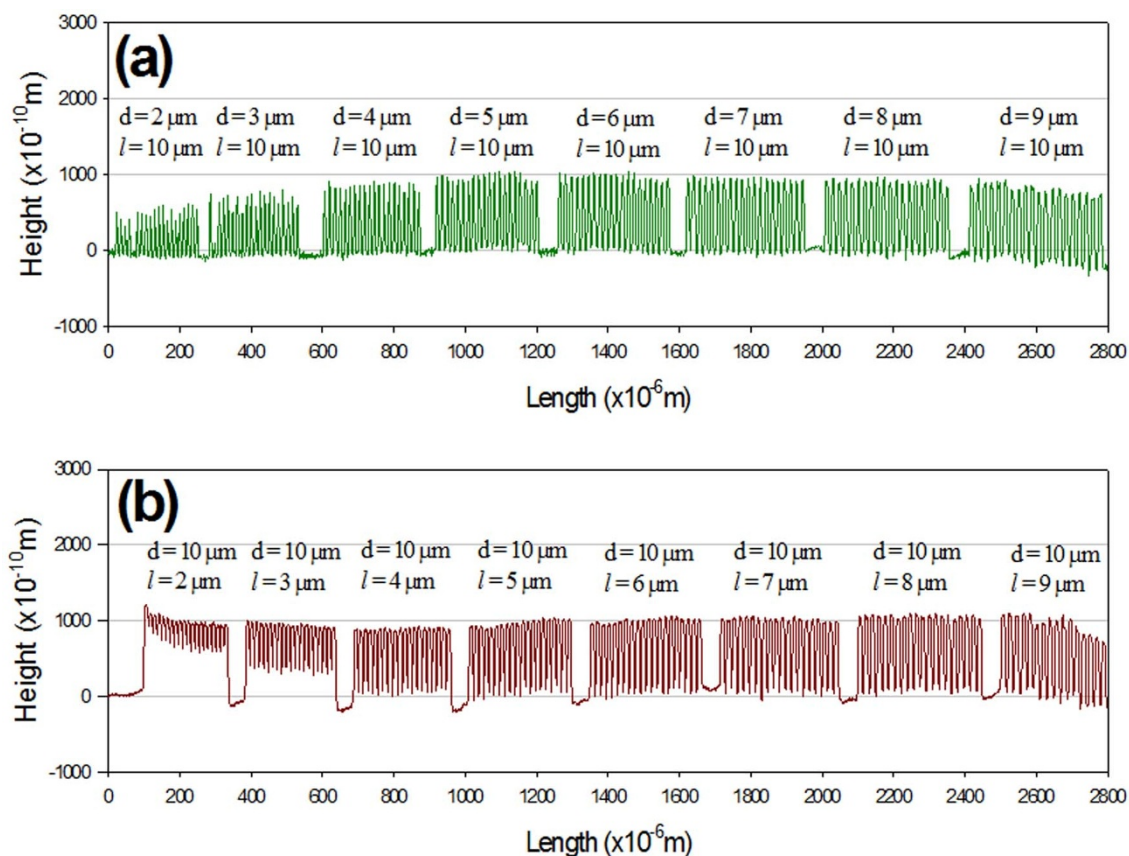


**Figure 4** | Alpha-step profiles of  $\text{TiO}_2$  thin films deposited on Si(100) substrates whose surface was patterned by (a) Pattern (1) and (b) Pattern (2).

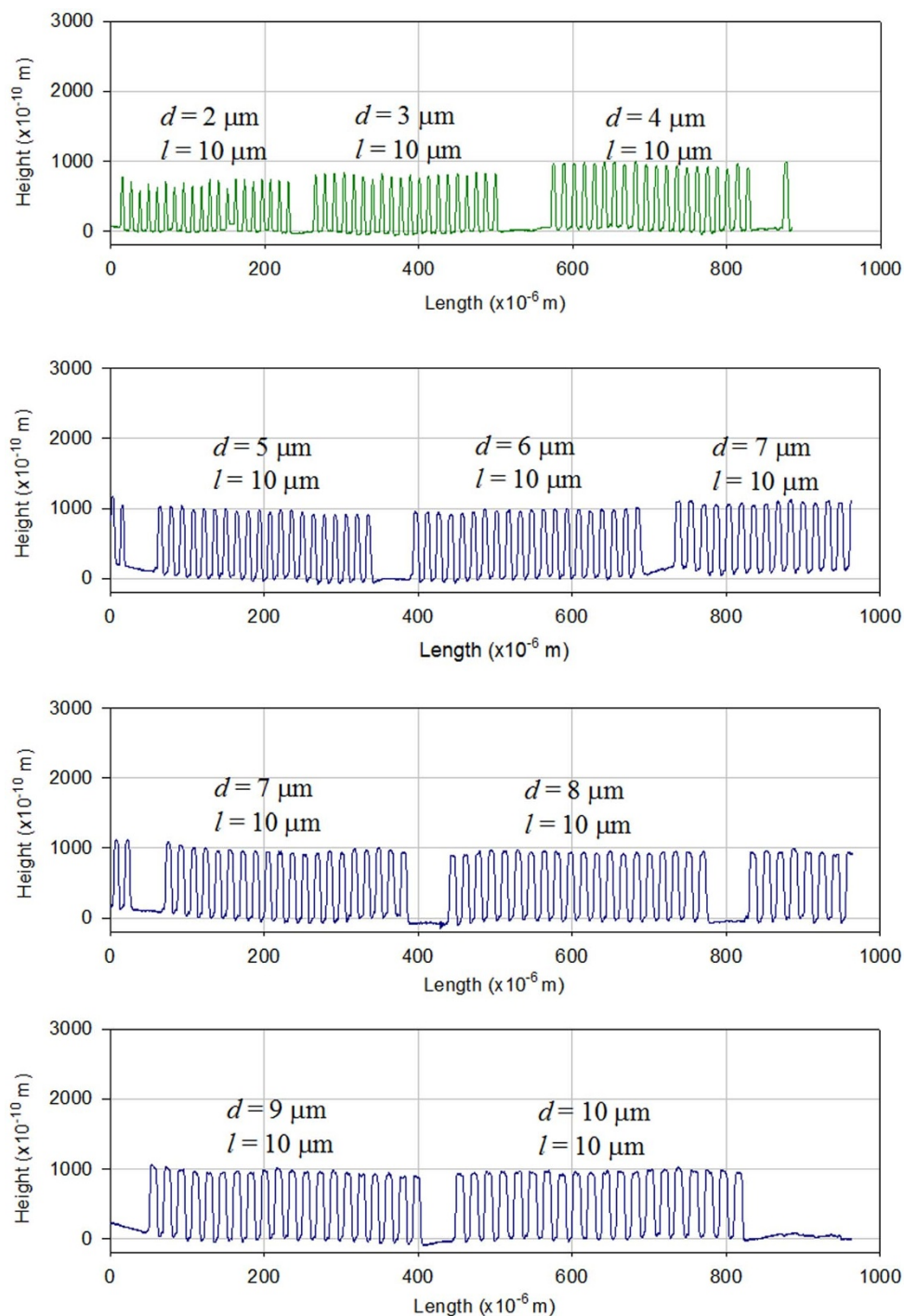


**Figure 5** | High resolution alpha-step profiles of deposited  $\text{TiO}_2$  thin films with various line-widths.

stripe MOCVD. However, in narrow stripe MOCVD, the MMR effect is not negligible, because the width of the growth stripe (less than  $2 \mu\text{m}$ ) is very similar to the dimension of the edge growth region<sup>12–14</sup>. If the migration effect of the precursor is effective, the thickness of the films grown on line-widths of less than under  $4 \mu\text{m}$  could be higher than that of line-widths over  $4 \mu\text{m}$ . However, in our experiment, the growth rate of the  $\text{TiO}_2$  thin film when the  $\text{TiO}_2$  was deposited on line-widths of less than  $4 \mu\text{m}$  was lower than that on line-widths of over  $4 \mu\text{m}$ . This means that the diffusion or migration effect of the precursors on the OTS SAMs regions was negligible, that is, there was no enhancement of the growth rate of the thin film resulting from the diffusion effect. Moreover, it was confirmed that the mask areas (OTS SAMs area) did not interfere with the process of

precursor diffusion, because there was no difference in the thickness of the deposited  $\text{TiO}_2$  thin film (Figure 7(b)). Because the terminal group of OTS is hydrophobic in nature, it could be very difficult for the precursor to diffuse and nucleate in order to grow the thin film. This means that the precursors which reached the OTS SAMs region are removed from the OTS region before the precursor diffuses on the OTS surface.

To find the main effect of the difference in growth rate between the narrow stripe area and wide stripe area, the mass flux of the precursor was considered. It can be considered that if the mass flux is fast in a certain area, the film deposition will be slow, because there is enough time for nucleation to take place for film formation. For this reason, a computer simulation experiment was also carried out. In order to

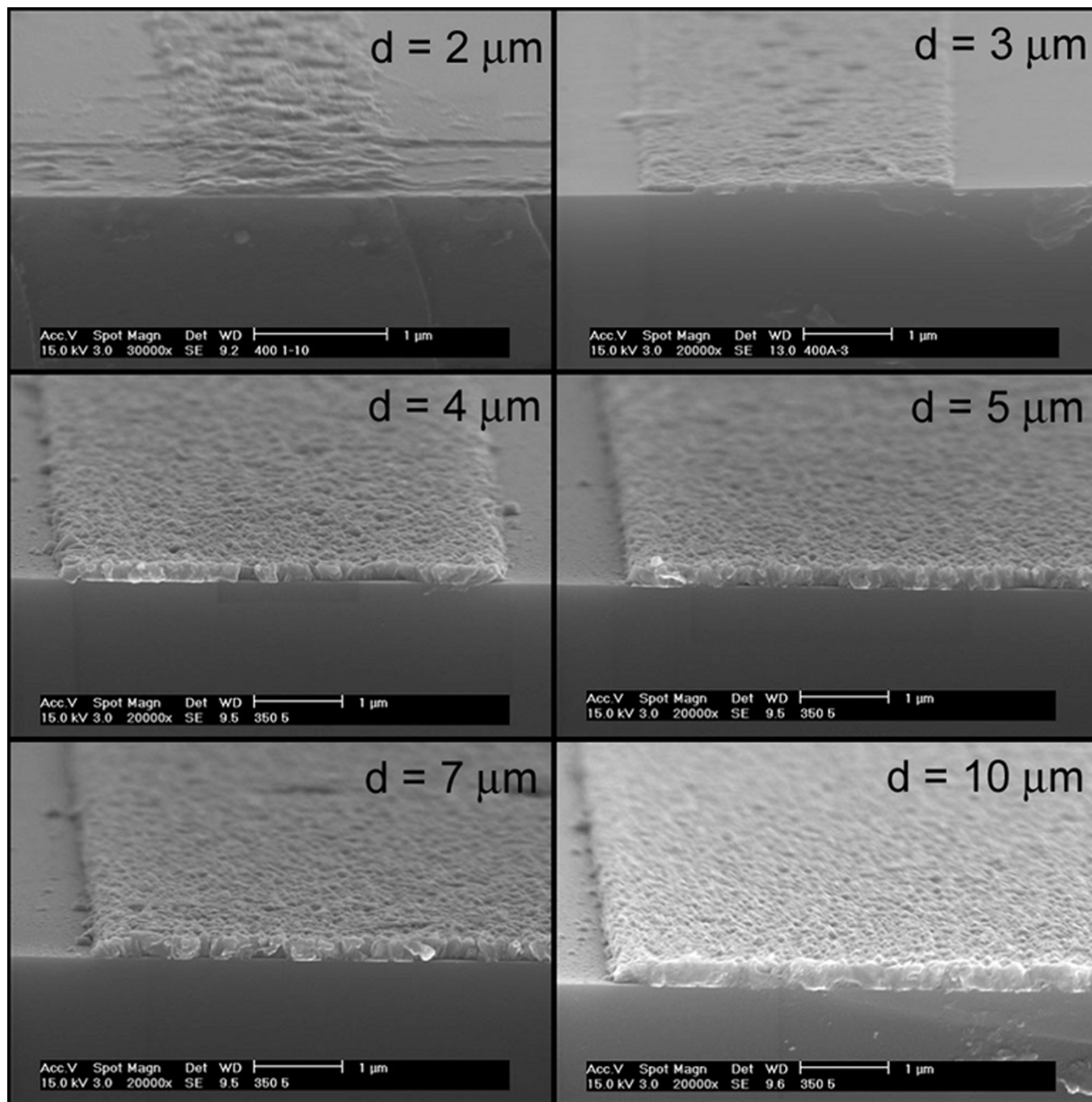


**Figure 6** | SEM images of  $\text{TiO}_2$  thin films deposited on OTS patterned Si(100) surfaces.

reveal the relationship between the  $\text{TiO}_2$  film thickness and deposited line width, we performed a numerical analysis using a commercial code, FLUENT 6.2.16. However, it is very difficult to solve the problem of a nano scale channel gas flow with a commercial code, so we used the *aspect ratio* of the channel width to height,  $\beta = W/H$ , in the range from 1 to 10, to solve a micro scaled channel gas flow problem. The Navier-Sokes governing equations which can be expressed as

$$\nabla \cdot (\rho \bar{v} \bar{v}) = -\nabla p + \nabla \cdot (\bar{\tau}) \quad \text{where} \quad \bar{\tau} = \mu \left[ \left( \nabla \bar{v} + \nabla \bar{v}^T \right) - \frac{2}{3} \nabla \cdot \bar{v} \mathbf{I} \right] \quad (2)$$

were used in this simulation test. As shown in Figure 9, gas flows along the channel. To compare the simulation with the experimental result, the analysis conditions were set to the same values as in the experiment. For example, the Reynolds number is calculated based

on the CVD diameter. The numerical results are shown in Figure 10. From the experimental results shown in Figure 8, we obtained the relationship between the film thickness and deposited line width,  $f(x) = a[1 - e^{(-bx)}]c$ . Comparing Figure 8 with Figure 10, it can be seen that the graph of the average mass flux in the flow direction has the reverse form of the experimental result, while that in the cross-flow direction has a similar form to the experimental data when the aspect ratio ( $\beta$ ) is less than 6 (see Figures 10(a) and 10(c)). This means that the velocity is directly related to the film thickness. As shown in Figure 10(a), when the aspect ratio,  $\beta$ , is over 6, the average mass flux values are almost equal and the film thickness of the experiment shows the same phenomenon. That is, when  $\beta$  is less than 5, the velocity is faster, so that the gas molecules do not stay long enough to be deposited. Therefore, the film thickness is decreased. However, when the average mass flux has a specific value, below  $1 \times 10^{-2}$ , the

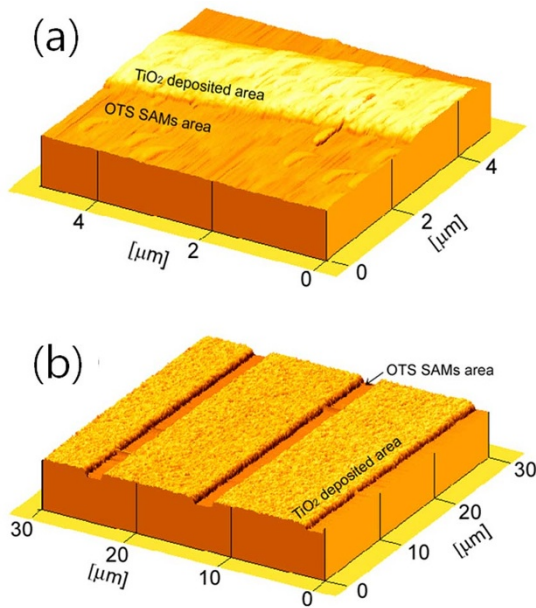


**Figure 7** | AFM images of TiO<sub>2</sub> thin films deposited on OTS patterned Si(100) surfaces. (a)  $d = 2 \mu\text{m}$ ,  $l = 10 \mu\text{m}$  and (b)  $d = 10 \mu\text{m}$ ,  $l = 2 \mu\text{m}$ .

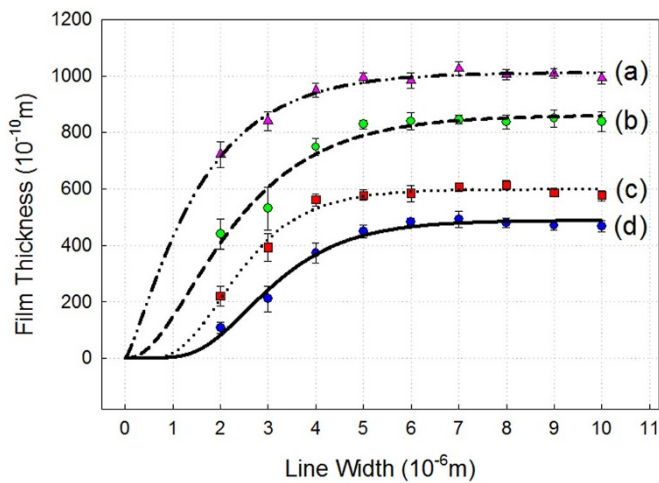


**Figure 8** | Thickness of TiO<sub>2</sub> thin film deposited on various line-width patterns. The deposition temperature was 350°C and the deposition time was (a) 2.5 hrs., (b) 2 hrs., (c) 1 hr. and (d) 0.5 hr.

gas molecules stay in the channel long enough to be deposited. But because of the growth rate and high average pressure in the flow direction (see Figure 10(b)), the increase of the film thickness is equal to each other when  $\beta$  is over 6.

In summary, the growth tendency of TiO<sub>2</sub> thin films deposited on a narrow-stripe area ( $< 10 \mu\text{m}$ ) was studied in this experiment. The experimental data showed that the film growth tendency was divided into two behaviors above and below a line patterning width of 4  $\mu\text{m}$ . The relationship between the film thickness and the deposited area

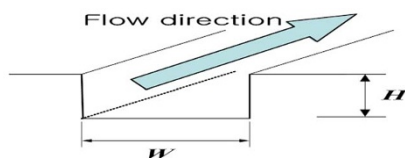
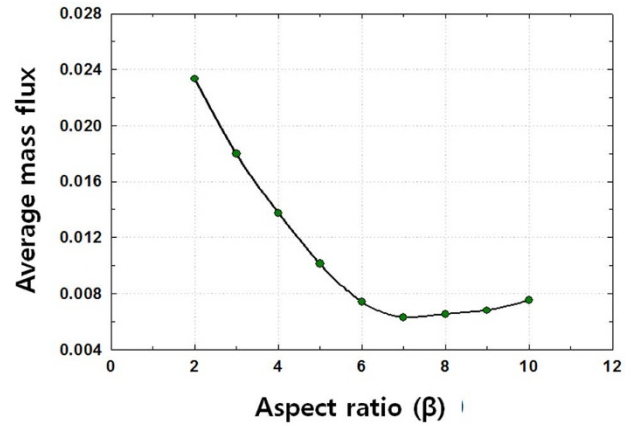
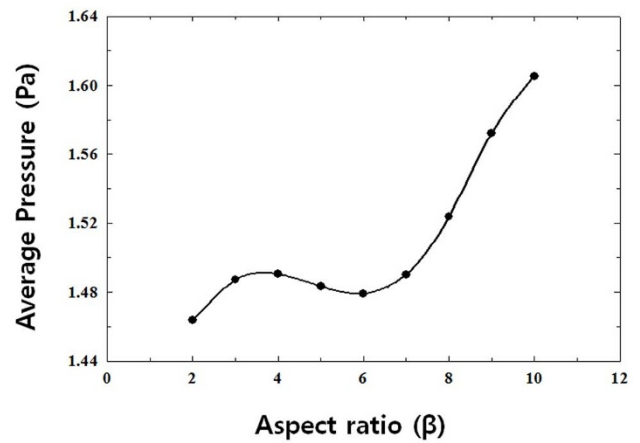


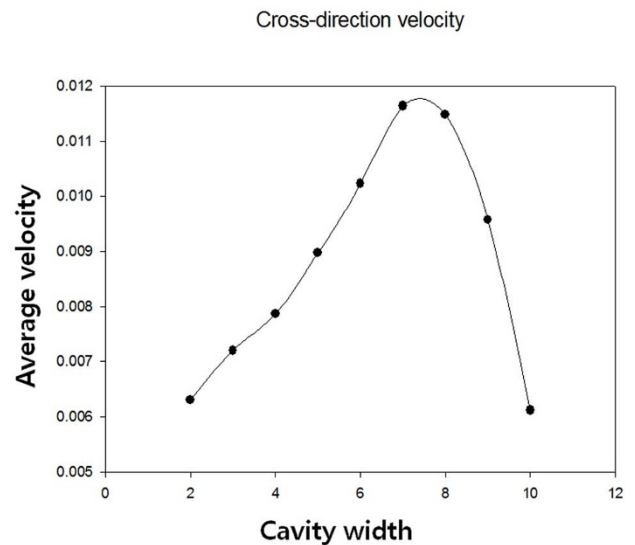
**Figure 9** | Schematic diagram of numerical model.



**(a)** Average mass (velocity) flux in flow direction



**(b)** Average pressure in flow direction



**(c)** Average velocity flux in cross-flow direction

**Figure 10** | Analysis results for cross-sectional area with various aspect ratios. (a) Average mass (velocity) flux in flow direction, (b) Average pressure in flow direction, and (c) Average mass (velocity) flux in cross-flow direction.

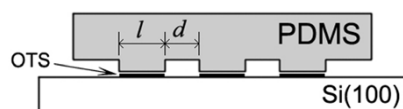


**Figure 11** | The PDMS stamp with narrow-stripe patterns. Two types of pattern were prepared. Pattern (1):  $l = 10 \mu\text{m}$ ,  $d = 2 \mu\text{m}$ – $10 \mu\text{m}$  (20 lines each) with  $1 \mu\text{m}$  space, Pattern (2):  $d = 10 \mu\text{m}$ ,  $l = 2 \mu\text{m}$ – $10 \mu\text{m}$  (20 lines each) with  $1 \mu\text{m}$  space.

was obtained as a function of  $f(x) = a[1 - e^{(-bx)}]c$ . The computer simulation experiment data suggested that the main effect of the difference in growth tendency depending on the linewidth was the average mass flux of the precursor on the narrow-stripe area substrate.

## Methods

**Preparation of alkylsiloxane SAMs.** Alkylsiloxane self-assembled monolayers (SAMs) were formed by immersing Si(100) substrates in a 2.5 mmol solution of octadecyltrichlorosilane [ $\text{CH}_3(\text{CH}_2)_{17}\text{SiCl}_3$ , (OTS)] precursor dissolved in hexadecane-chloroform (4 : 1). The samples were then washed in carbon tetrachloride to remove the excess reactants and dried with nitrogen gas.

**Preparation of patterned SAMs using microcontact printing.** A patterned monolayer of OTS was formed on the Si(100) substrates by the microcontact printing method. Masters were fabricated using conventional photo-lithography or the e-beam lithographic method to pattern resists on the Si wafers. The masters have parallel lines and spaces with dimensions in the range from 10 to  $1 \mu\text{m}$ . Polydimethylsiloxane (PDMS) stamps were produced according to a previously reported procedure<sup>3–5</sup>. The PDMS stamps were inked with a 10 mM hexane solution of OTS and dried with nitrogen gas. The PDMS stamps was placed in contact with the Si(100) substrates at 298 K for 30 s, then carefully peeled off and dried with nitrogen gas.

**Selective growth of  $\text{TiO}_2$  thin film by MOCVD.**  $\text{TiO}_2$  thin films were selectively deposited on OTS patterned Si(100) substrates by MOCVD using titanium(IV) isopropoxide [ $\text{Ti}(\text{OiPr})_4$ ] as a single molecular precursor. No carrier or reactive gas was used. The OTS patterned Si(100) substrate was cleaned with ethanol and de-ionized water in an ultrasonic cleaner without acid treatment to protect the OTS layer. The deposition was performed in a homemade MOCVD apparatus<sup>15</sup>. The base pressure of the MOCVD apparatus was  $1.0 \times 10^{-3}$  Torr and the working pressure was kept at  $3.0 \times 10^{-2}$  Torr. The deposition was carried out at  $350^\circ\text{C}$  for 0.5–2.5 hrs.

**Design & fabrication of PDMS stamps with different line patterns.** In order to investigate the growth tendency of the films deposited on the narrow parallel line pattern area, PDMS stamps were designed and fabricated according to a previously reported procedure<sup>5,16</sup>. Figure 11 shows the PDMS stamps with narrow parallel line patterns. The stamps contained two different types of line patterns. Pattern (1):  $l = 10 \mu\text{m}$ ,  $d = 2 \mu\text{m}$ – $10 \mu\text{m}$  (20 lines each) with  $1 \mu\text{m}$  space, Pattern (2):  $d = 10 \mu\text{m}$ ,  $l = 2 \mu\text{m}$ – $10 \mu\text{m}$  (20 lines each) with  $1 \mu\text{m}$  space. These patterns were transferred to the Si(100) surface by the microcontact printing method using OTS solution as the ink for the formation of self-assembly monolayers on the Si(100) surfaces.

- Xia, Y., Rogers, J. A., Paul, K. A. & Whitesides, G. Unconventional Methods for Fabricating and Patterning Nanostructures. *Chem. Rev.* **99**, 1823–1848 (1999).
- Kumar, A., Biebuyck, H. A., Abbott, N. L. & Whitesides, G. The use of self-assembled monolayers and a selective etch to generate patterned gold features. *J. Am. Chem. Soc.* **114**, 9188–9189 (1992).
- Kumar, A. & Whitesides, G. Features of gold having micrometer to centimeter dimensions can be formed through a combination of stamping with an elastomeric stamp and an alkanethiol “ink” followed by chemical etching. *Appl. Phys. Lett.* **63**, 2002–2005 (1993).

- Kumar, A., Biebuyck, H. A. & Whitesides, G. Patterning Self-Assembled Monolayers: Applications in Materials Science. *Langmuir* **10**, 1498–1511 (1994).
- Kang, B.-C. *et al.* Selective growth of  $\text{TiO}_2$  thin films on Si(100) surfaces by combination of metalorganic chemical vapor deposition and microcontact printing methods. *J. Vac. Sci. Technol.* **21**, 1773–1776 (2003).
- Folch, A. & Schmidt, M. A. Wafer-Level In-Registry Microstamping. *IEEE J. of Microelectromechanical Systems* **8**, 85–89 (1999).
- Sun, C. & d. Xue, D. Tailoring Anisotropic Morphology at the Nanoregime: Surface Bonding Motif Determines the Morphology Transformation of ZnO Nanostructures. *J. of Phys. Chem.* **C117**, 5505–5511 (2013).
- Xue, D., Li, K., Liu, J., Sun, C. & Chen, K. Crystallization and functionality of inorganic materials. *Mats. Res. Bull.* **47**, 2838–2842 (2012).
- Sun, C. & Xue, D. Chemical bonding theory of single crystal growth and its application to  $\Phi 3^\circ$  YAG bulk crystal. *Crystengcomm* **16**, 2129–2135 (2014).
- Sun, C., Song, S., Xue, D. & Zhang, H. CRYSTALLIZATION OF OXIDES AS FUNCTIONAL MATERIALS. *Functional Materials Letters* **5**, 12300021–123000217 (2012).
- Sakata, Y., Inomoto, Y. & Komatu, K. Surface migration effect and lateral vapor-phase diffusion effect for InGaAsP/InP narrow-stripe selective metal-organic vapor-phase epitaxy. *J. Crystal Growth* **208**, 130–136 (2000).
- Yamaguchi, K., Ogasawara, M. & Koamoto, K. Surface diffusion model in selective metalorganic chemical vapor deposition. *J. Appl. Phys.* **72**, 5919–5925 (1992).
- Xia, Y. & Whitesides, G. Soft Lithography. *Angew. Chem. Int. Ed.* **37**, 550–575 (1998).
- Park, K. S., Seo, E. K., Do, Y. R., Kim, K. & Sung, M. M. Light Stamping Lithography: Microcontact Printing without inks. *J. Am. Chem. Soc.* **128**, 859–865 (2006).
- Kang, B.-C., Lee, S.-B. & Boo, J.-H. Growth of  $\text{TiO}_2$  thin films on Si(100) substrates using single molecular precursors by metal organic chemical vapor deposition. *Surface and Coatings Technology* **31**, 88–92 (2000).
- Park, M. H., Jang, Y. J., Sung-Suh, H. M. & Sung, M. M. Selective Atomic Layer Deposition of Titanium Oxide on Patterned Self-Assembled Monolayers Formed by Microcontact Printing. *Langmuir* **20**, 2257–2260 (2004).

## Acknowledgments

This research was supported by the Basic Science Research Program through the National Research Foundation (NRF) of Korea founded by the Ministry of Education (2010-0025481). This work was also supported by a grant from the Human Resources Development program (No. 20124010203280) of the Korea Institute of Energy Technology Evaluation and Planning (KETEP) funded by the Korea government Ministry of Trade, Industry and Energy.

## Author contributions

Y.J.K., D.-Y.J. and J.-H.B. conceived this project. Y.J.K. and J.-H.B. evaluated the experimental results as well as doing the computer simulation. K.-H.H. and B.-C.K. performed all of the experiments. B.-C.K., Y.J.K. and J.-H.B. wrote the manuscript, and all of the other authors contributed to its editing.

## Additional information

**Competing financial interests:** The authors declare no competing financial interests.

**How to cite this article:** Hwang, K.-H., Kang, B.-C., Jung, D.Y., Kim, Y.J. & Boo, J.-H. Micropatterning of  $\text{TiO}_2$  Thin Films by MOCVD and Study of Their Growth Tendency. *Sci. Rep.* **5**, 9319; DOI:10.1038/srep09319 (2015).



This work is licensed under a Creative Commons Attribution-NonCommercial-NoDerivs 4.0 International License. The images or other third party material in this article are included in the article's Creative Commons license, unless indicated otherwise in the credit line; if the material is not included under the Creative Commons license, users will need to obtain permission from the license holder in order to reproduce the material. To view a copy of this license, visit <http://creativecommons.org/licenses/by-nc-sa/4.0/>